Electronic Supplementary Material (ESI) for Catalysis Science & Technology.
This journal is © The Royal Society of Chemistry 2021

Electronic Supplementary Information

Green light (550 nm) driven tunable syngas synthesis from CO_2 photoreduction using heterostructured layered double hydroxide/TiC photocatalysts

Huijuan Wang,‡[a] Sha Bai,‡[a] Pu Zhao,[b] Ling Tan,[a] Chenjun Ning,[a] Guihao Liu,[a] Jikang Wang,[a] Tianyang Shen,[a] Yufei Zhao*[a] and Yu-Fei Song*[a]

[a] State Key Laboratory of Chemical Resource Engineering, Beijing Advanced Innovation Center for Soft Matter Science and Engineering, Beijing University of Chemical Technology, Beijing 100029 P. R. China.

[b] Department of Chemistry, University of Oxford, Oxford OX1 3QR, U.K

* Corresponding author

Email: songyf@mail.buct.edu.cn, zhaoyufei@mail.buct.edu.cn. Tel/Fax: +86 10 64431832

‡ These authors contributed equally to this work.

Experimental:

Materials: $Al(NO_3)_3 \cdot 9H_2O$, $Mg(NO_3)_2 \cdot 6H_2O$, $Co(NO_3)_2 \cdot 6H_2O$, TiC, NaOH, Triethanolamine (TEOA), acetonitrile (MeCN) were purchased from Sigma-Aldrich Co. All drugs can be used without further purification and deionized water was used in all experiments.

Synthesis of CoMgAl-LDH nanosheets (denoted as LDH):

The LDH nanosheets were synthesis by a simple co-precipitation method. LDH was synthesized directly by adding a 20.0 mL solution consisting of 3.30 mM $Al(NO_3)_3 \cdot 9H_2O$, 6.39 mM $Mg(NO_3)_2 \cdot 6H_2O$, and 0.21 mM $Co(NO_3)_2 \cdot 6H_2O$ drop by drop into 20 mL of the aqueous solution. Meanwhile, 0.25 M NaOH was added, and the pH value of the system was kept at ~ 10 and the temperature was maintained at 80℃ under magnetic agitation. The reaction was completed in 10 minutes. The precipitation was collected by centrifugation and washed with water more than 3 times, and finally dried at 60 °C.

Synthesis of CoMgAl-LDH/TiC-*x* (*x* refers to the weight ratio of LDH to TiC, there in, x= 1.7, 1.2, 1.0) nanosheets (denoted as LDH/TiC-*x*):

The LDH/TiC-1.7 nanosheets were synthesis by a simple double-drop method. At first, TiC (1.5 g) was added to 150 mL H_2O and ultrasonicated for 5h. LDH/TiC-1.7 was synthesized directly by adding a 20 mL solution of a solution consisting of 0.007 mM $Al(NO_3)_3 \cdot 9H_2O$, 0.013 mM $Mg(NO_3)_2 \cdot 6H_2O$, and 0.410 mM $Co(NO_3)_2 \cdot 6H_2O$ drop by drop into to 20 mL of 10 mg/mL TiC solution. Meanwhile, 0.25 M NaOH was added, and the pH value of the system was kept at ~ 10 and the temperature was maintained at 80°C under magnetic agitation. The reaction was completed in 10 minutes. The precipitation was collected by centrifugation and washed with water more than 3 times.

The CoMgAl-LDH/TiC-1.2 (denoted as LDH/TiC-1.2) and CoMgAl-LDH/TiC-1.0 (denoted as LDH/TiC-1.0) were synthesized by the same method, but the composition of the solution was changed. LDH/TiC-1.2 was synthesized from 20 mL solution of 0.005 mM $Al(NO_3)_3 \cdot 9H_2O$, 0.010 mM $Mg(NO_3)_2 \cdot 6H_2O$ and 0.005 mM $Co(NO_3)_2 \cdot 6H_2O$ and 20 mL solution of 10 mg/mL TiC. LDH/TiC-1.0 was synthesized from 20 mL solution of 3.30 mM $Al(NO_3)_3 \cdot 9H_2O$, 6.39 mM $Mg(NO_3)_2 \cdot 6H_2O$ and 0.21 mM $Co(NO_3)_2 \cdot 6H_2O$ and 20 mL solution of 10 mg/mL TiC.

Electrochemical Test

Electrochemical impedance spectroscopy (EIS) and the transient photocurrent response were performed on an electrochemical system (CHI760A, Shanghai Chenhua, China) with a standard three-electrode quartz cell. An Ag/AgCl electrode and platinum (Pt) wire were used as a reference and a counter electrode, respectively. For the electrochemical impedance spectroscopy (EIS) experiment, LDH, LDH/TiC-1.2, and TiC were used as electrodes in 1.0 M KOH aqueous solution (electrolyte solution) at room temperature. Powder sample-based electrodes were made by the following steps: 5 mg of LDH, LDH/TiC-1.2, or TiC powders were dispersed in 1 mL of ethanol to form catalyst ink. The distance between the counter and the working electrode was 2 cm. The carbon-fiber paper loading 1.05 mg photocatalyst within 1×1 cm area was served as a working electrode. The transient photocurrent response was measured in a Na_2SO_4 solution (0.1 M) with a 300 W Xe lamp under a 400 nm cutoff filter (400−800 nm) as the light source. A sample (25 mg) was completely dispersed in a 1 mL solution of CH_3CH_2OH/H_2O = 3:7 (v/v). Subsequently, the obtained slurry (80 μL) was dropped onto the ITO glass with an area of 1 cm × 1 cm as the working electrode.

Table S1. The performance of various photocatalysts for photocatalytic CO_2 reduction is compared in this work and the previous literature.

Catalyst	Photosensitizer Co-catalyst	Sacrificial agent	Solvent	Light source	Major product evolution rate ($\mu mol \bullet h^{-1} \bullet g^{-1}$)	Ref.
LDH	**$Ru(bpy)_3Cl_2 \cdot 6H_2O$**	**TEOA**	**MeCN-H_2O-TEOA (3:1:1 v/v/v)**	**300 W Xe (λ > 400 nm)**	**CO: 956.63 H_2: 1021.05**	**This work**
LDH/TiC (1.7-1.0)	**$Ru(bpy)_3Cl_2 \cdot 6H_2O$**	**TEOA**	**MeCN-H_2O-TEOA (3:1:1 v/v/v)**	**300 W Xe (λ > 400 nm)**	**CO: 741.07 - 303.97 H_2: 1084.64 - 780.24**	**This work**
TiC	**$Ru(bpy)_3Cl_2 \cdot 6H_2O$**	**TEOA**	**MeCN-H_2O-TEOA (3:1:1 v/v/v)**	**300 W Xe (λ > 400 nm)**	**CO: 287.13 H_2:1011.89**	**This work**
LDH/TiC	**$Ru(bpy)_3Cl_2 \cdot 6H_2O$**	**TEOA**	**MeCN-H_2O-TEOA (3:1:1 v/v/v)**	**300 W Xe (λ = 550 nm)**	**CO:534.13 - 203.06 H_2: 813.85 - 368.59**	**This work**
LDH/TiC-1.2	**$Ru(bpy)_3Cl_2 \cdot 6H_2O$**	**4-Bromobenzyl alcohol**	**MeCN-H_2O-TEOA (3:1:1 v/v/v)**	**300 W Xe (λ > 400 nm)**	**CO: 23**	**This work**
Co-ZIF-9	$Ru(bpy)_3Cl_2 \cdot 6H_2O$	TEOA	MeCN-H_2O-TEOA (4:1:1 v/v/v)	300 W Xe (λ > 420 nm)	CO: 41.8 H_2: 30.3	Angew. Chem. Int. Ed., 2014, 53[1]
Co_3O_4-400	$Ru(bpy)_3Cl_2 \cdot 6H_2O$	TEOA	MeCN-H_2O (3:1 v/v)	300 W Xe (λ > 420 nm)	CO: 2003 H_2: 595	Adv. Mater., 2016, 28[2]

$[Co_2(OH)L^1](ClO_4)_3$	$[Ru(phen)_3](PF_6)_2$	TEOA	MeCN-H_2O (4:1 v/v)	LED (λ = 450 nm)	CO: 2.11 H_2: 0.046	Angew. Chem. Int. Ed., 2017, 56[3]
MAF-X27l-OH	$Ru(bpy)_3Cl_2 \cdot 6H_2O$	TEOA	MeCN-H_2O (4:1 v/v)	LED (λ = 420 nm)	CO: 45 H_2: 0.8	JACS, 2018, 140[4]
Co-G nanosheets	$Ru(bpy)_3Cl_2 \cdot 6H_2O$	TEOA	MeCN-H_2O (3:1 v/v)	300 W Xe (λ > 420 nm)	CO: 59299 H_2: 15384	Adv. Mater., 2018, 1704624[5]
Co/C	$Ru(bpy)_3Cl_2 \cdot 6H_2O$	TEOA	MeCN-H_2O-TEOA (3:1:1 v/v/v)	300 W Xe (λ > 450 nm)	CO: 448 H_2: 250	Small, 2018, 14[6]
Pd/CoAl-7.57	$Ru(bpy)_3Cl_2 \cdot 6H_2O$	TEOA	MeCN-H_2O-TEOA (3:1:1 v/v/v)	300 W Xe (λ > 400 nm)	CO: 581.8 H_2: 1299.1	J. Energy. Chem, 2020, 46[7]
(Co/Ru)n-UiO-67(bpydc)	-	TEOA	CH_3CN/H_2O (9/1, v/v)	LED (λ = 450 nm)	CO: 570.09 H_2: 282.5	Appl. Catal. B, Environ., 2019, 245[8]
MAF-X27/-OH	$Ru(bpy)_3Cl_2 \cdot 6H_2O$	TEOA	MeCN-H_2O (4:1 v/v)	LED (λ = 420 nm)	CO: 45 H_2: 0.8	JACS, 2018, 140, 38[4]
MoO(dithiolene)$_2$ complex	$Ru(bpy)_3Cl_2 \cdot 6H_2O$	BIH	MeCN-TEOA (5:1 v/v	300 W Xe (λ = 400 -1200 nm)	HCOOH: (39%) CO: (19%) H_2: (42%)	Angew. Chem. Int. Ed., 2018, 57, 17033[9]
g-C_3N_4	$Co(bpy)_3^{2+}$	TEOA	MeCN-H_2O (4:1 v/v)	300 W Xe (λ > 420 nm)	CO: 469 H_2: 104	Appl. Catal. B, 2015, 179, 1[10]

LDH/MoS_2 (0.2 - 1.5 mg/mL)	$Ru(bpy)_3Cl_2 \cdot 6H_2O$	TEOA	MeCN-H_2O-TEOA (3:1:1 v/v/v)	300 W Xe (λ > 400 nm)	CO: 1415-219 H_2: 3211-1821	Chem. Commun, 2020, 56[11]

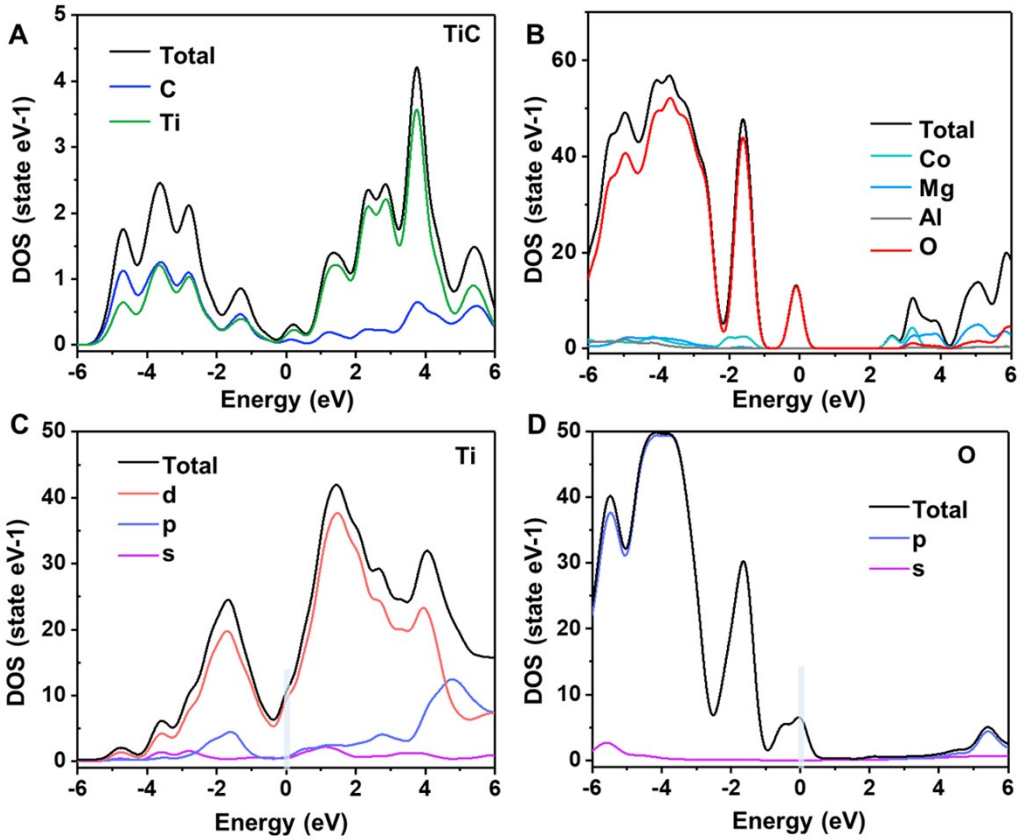

Figure S1. The calculated density of states (DOS) of (A) TiC, (B) LDH, (C) Ti and (D) O in LDH/TiC.

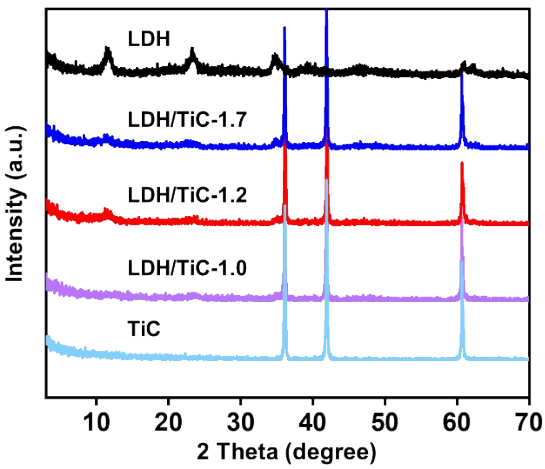

Figure S2. XRD patterns of LDH, CoMgAl-LDH/TiC-*x* (*x* refers to the weight ratio of LDH to TiC, there in, *x*= 1.7, 1.2, 1.0), TiC, respectively.

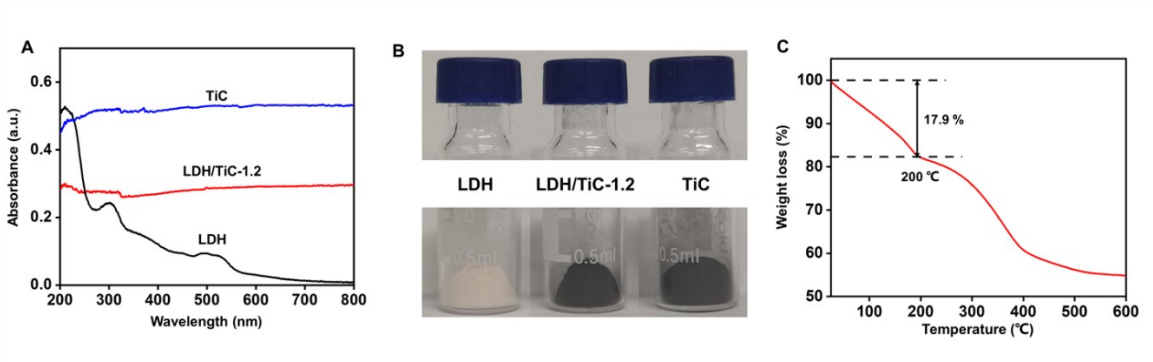

Figure S3. A) UV-visible spectra and B) Digital photographs of LDH, LDH/TiC-1.2, and TiC; C) TG curve of LDH.

As shown in Figure S3A, the absorption band at 460-560 nm of CoMgAl-LDH can be contributed to the d-d transitions of octahedral Co^{2+}, as originated to the $^4T_{1g}$ (F) → $^4T_{1g}$ (P).

Table S2. ICP results of LDH/TiC-1.7, LDH/TiC-1.2 and LDH/TiC-1.0.

	LDH/TiC ratio
LDH/TiC-1.7	1.7
LDH/TiC-1.2	1.2
LDH/TiC-1.0	1.0

The general formula for the structure of Layered double hydroxides (LDHs) is $[M^{2+}_{1-x}M^{3+}_{x}(OH)_2]^{x+}(A^{n-})_{x/n}\cdot mH_2O$[12], where M^{2+} and M^{3+} are divalent and trivalent metal cations, located on the theme lamination, A^{n-} is an interlayer anion, *x* is the mole ratio of $M^{3+}/(M^{2+}+M^{3+})$ and according to ICP results, the molar ratio of $M^{3+}/(M^{2+}+M^{3+})$ is 0.314. m is the number of water molecules between LDH layers. Further, according to (thermogravimetric) TG results (Figure S3C), the TG showed two steps of consecutive weight-loss, the first step from 25 to 200 °C corresponding to the loss of intercalated water molecules[13]. Therefore, we can get that the content of H_2O in LDH structure is 0.85. According to the ICP and TG results, the structural formula of LDH can be obtained as $[Co_{0.022}Mg_{0.664}Al_{0.314}(OH)_2]^{0.314+}$ $(CO_3^{2-})_{0.157}\cdot 0.85H_2O$. The structural formula for TiC is known. Thus, we can calculate the ratio of CoMgAl-LDH and TiC in the catalyst. We can calculate the actual measurement results (PPb) of Ti with ICP-AES, and further calculate the amount of TiC in the 10 mg catalyst. The LDH content can be obtained by subtracting the amount of TiC from the 10 mg catalyst (LDH=10-TiC(mg)).

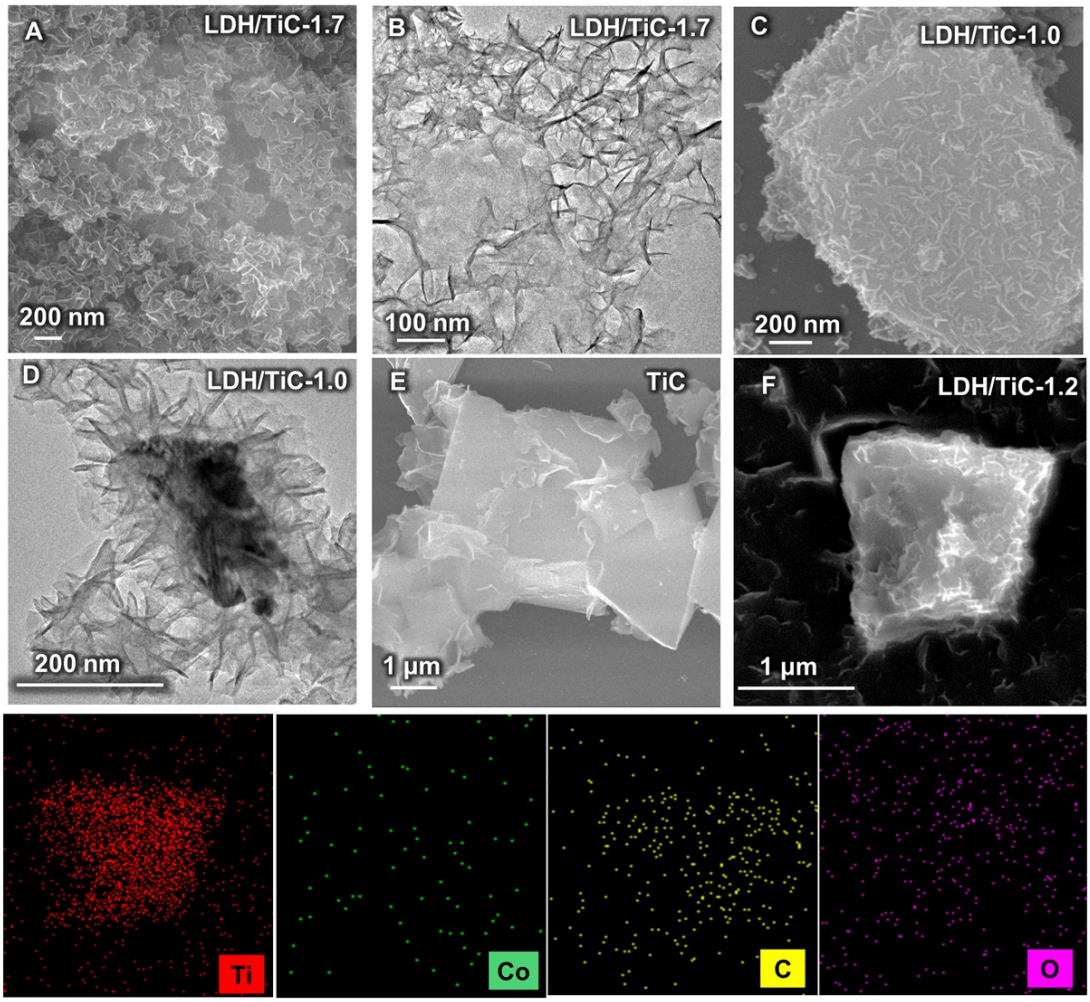

Figure S4. A) SEM image of LDH/TiC-1.7; B) TEM image of LDH/TiC-1.7; C,D) SEM and TEM images of LDH/TiC-1.0; E) SEM image of TiC; F) EDS mapping images of LDH/TiC-1.2.

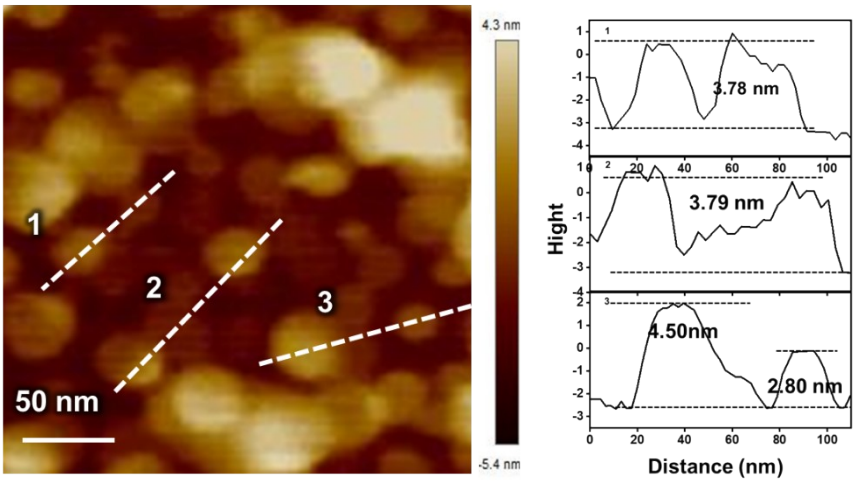

Figure S5. AFM image and height profiles of LDH.

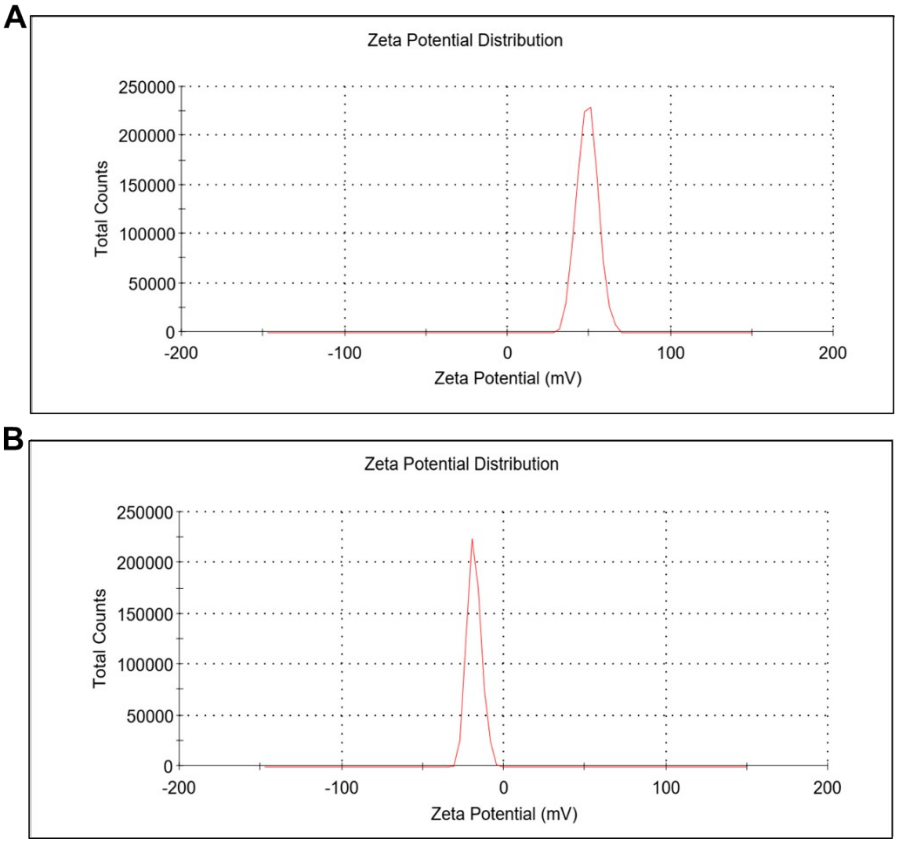

Figure S6. Zeta potentials of (A) LDH, (B) TiC, samples dispersed in water.

Table S3. Zeta potentials of LDH and TiC.

Simple	Zeta potential (mV)
LDH	+48.7
TiC	-18.3

As shown in Figure S6 and Table S3, the zeta potential was measured with water as the solvent (pH=7). For Zeta potential test, 5 mg LDH and 5 mg TiC were dispersed in 5 mL H_2O, respectively. Zeta potential of LDH was positively charged (+48.7 mV), and TiC was negatively charged (-18.3 mV), indicating that LDH/TiC was bound by electrostatic interaction (Table S3).

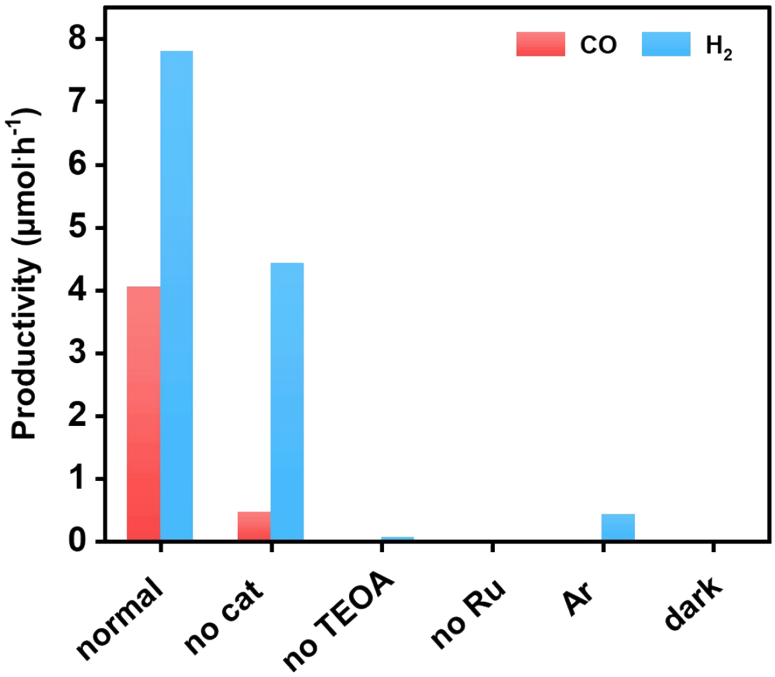

Figure S7. Photocatalytic CO_2 reduction performance of different reaction systems.

Table S4. The amount of LDH and TiC in the physical mixture of 10 mg catalyst under the same irradiation conditions.

	LDH/mg	TiC/mg	LDH+TiC (LDH/TiC mg/mg)
LDH+TiC-2.3	7.00	3.00	2.3
LDH+TiC-1.7	6.23	3.77	1.7
LDH+TiC-1.2	5.40	4.60	1.2
LDH+TiC-1.0	4.90	5.10	1.0
LDH+TiC-0.7	4.00	6.00	0.7

To determine the difference between physical mixing and chemical action in photocatalysis, the photocatalytic experiments of LDH+TiC-2.3, LDH+TiC-1.7, LDH+TiC-1.2, LDH+TiC-1.0, and LDH+TiC-0.7 were carried out according to the ICP results (Table S4).

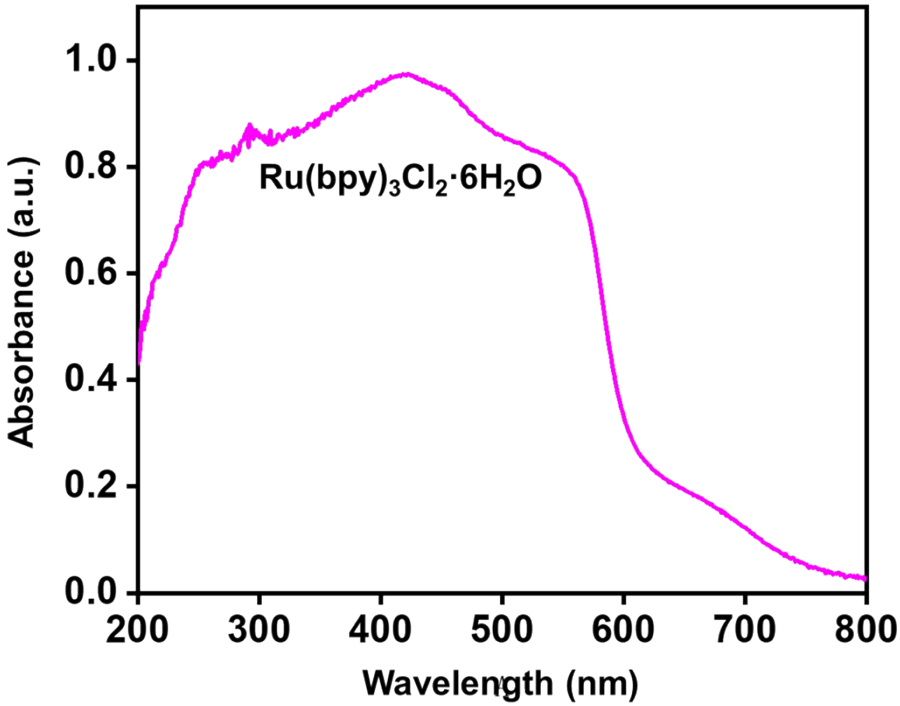

Figure S8. UV-visible spectra of the photosensitizer $Ru(bpy)_3Cl_2 \cdot 6H_2O$.

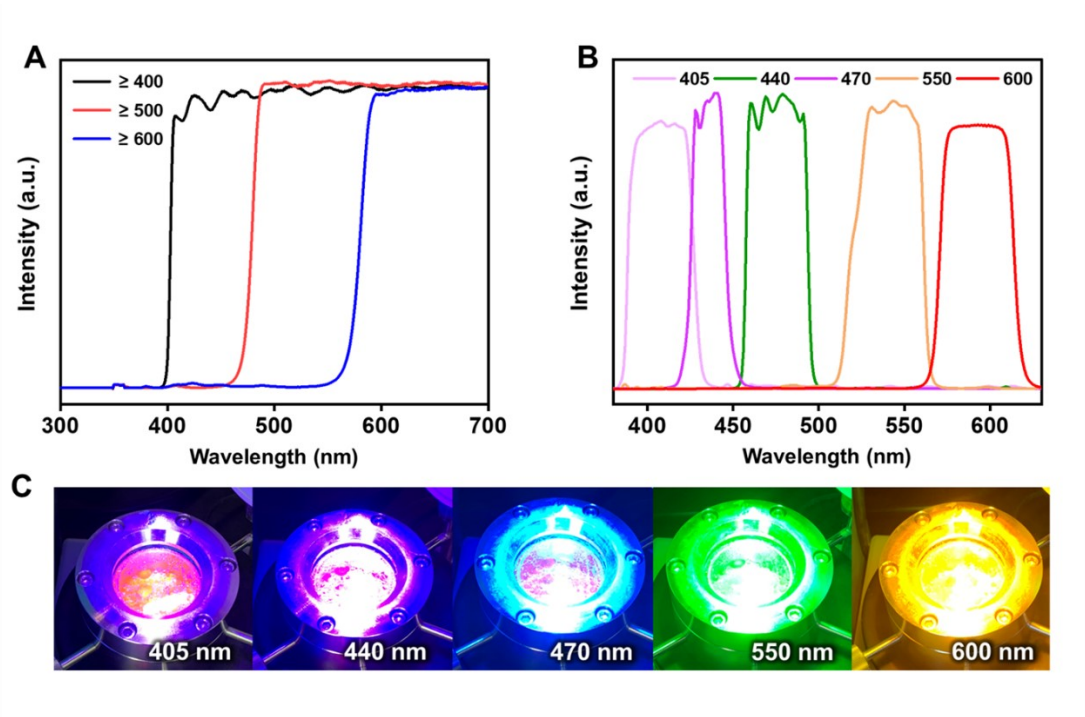

Figure S9. A) The wavelength range for the optical cutoff filter; B) the range of wavelengths of monochromatic light; C) different optical cutoff filters for optical photographs.

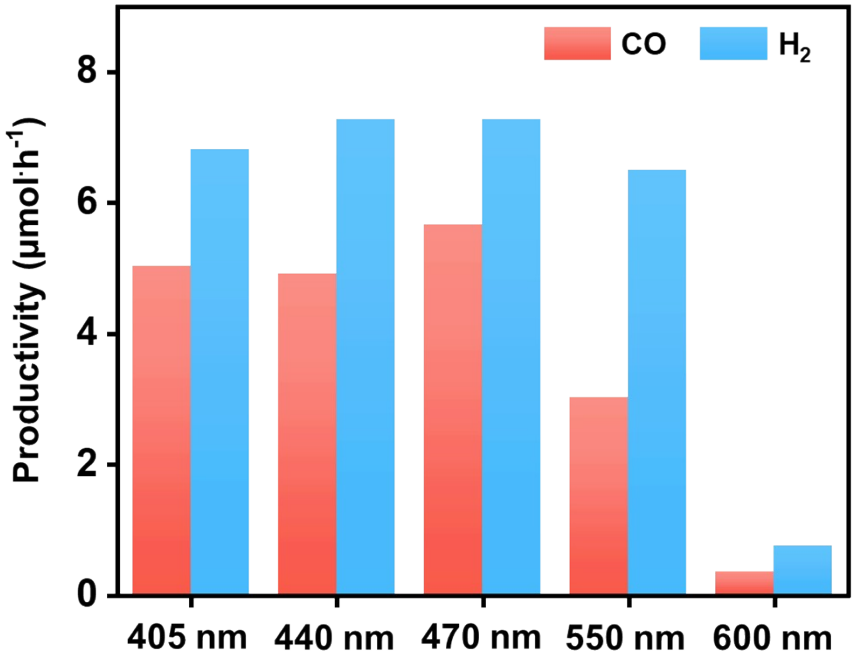

Figure S10. The productivity of CO and H_2 in CO_2PR on LDH/TiC-1.2 under different monochromatic light.

Table S5. The AQY values were generated by CO irradiation with different monochromatic wavelengths using LDH/TiC-1.2 (10 mg).

Wavelength (nm)	Optical density (mW/cm^2)	AQY_{CO}(%)
405	79	1.33
470	88	1.16
550	96	0.48
600	136	0.04

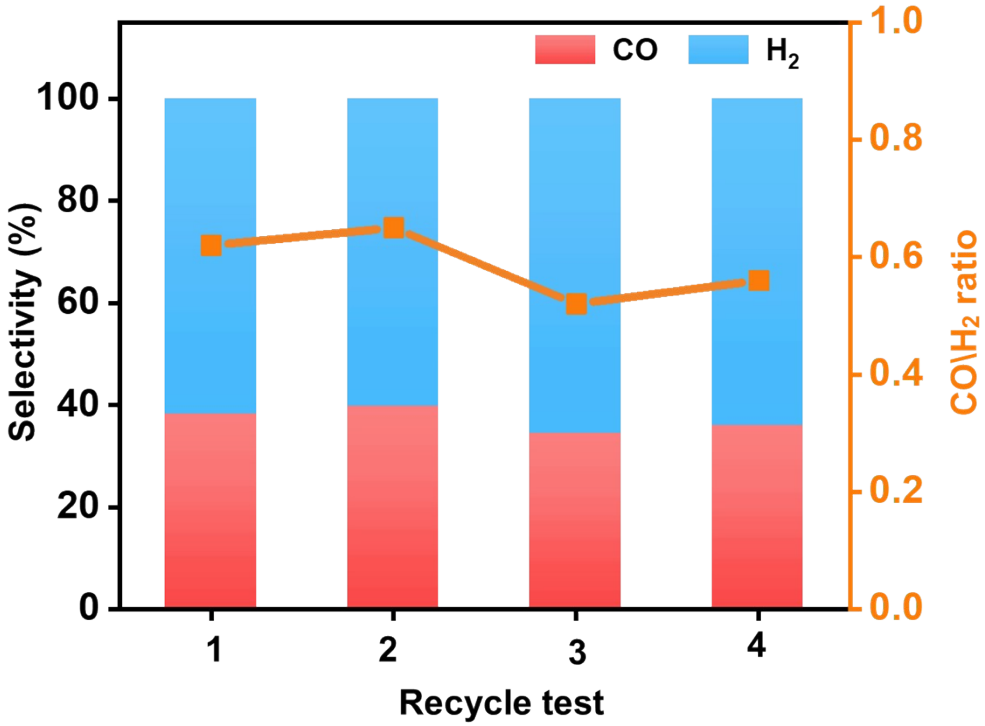

Figure S11. The selectivity of CO and H_2 on LDH/TiC-1.2 (10 mg) for four consecutive photocatalytic experiments.

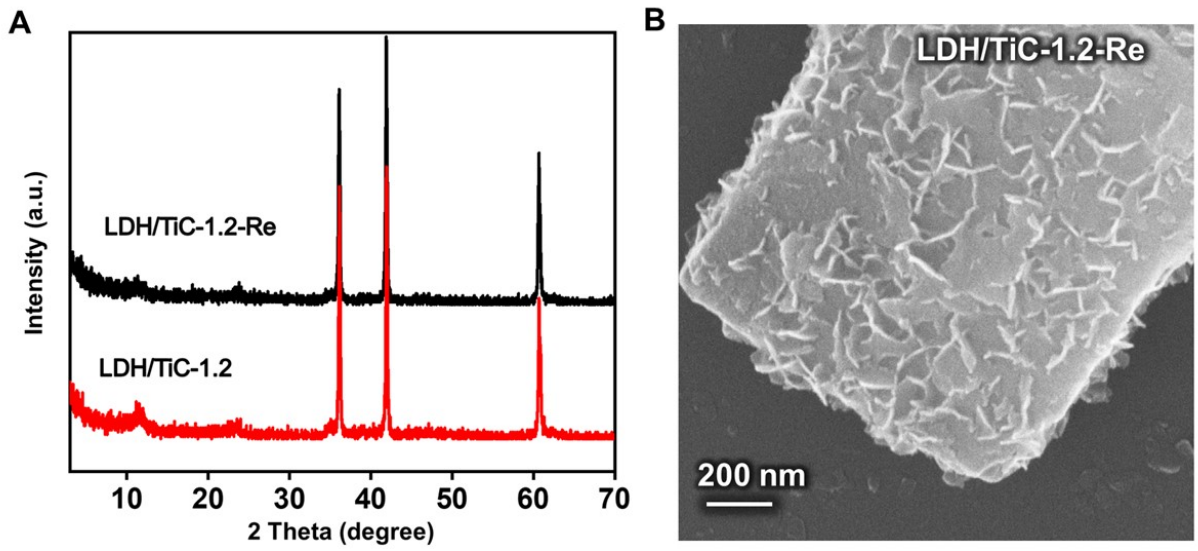

Figure S12. A) XRD patterns of LDH/TiC-1.2 fresh and after photocatalytic reaction; B) SEM image of the LDH/TiC-1.2 after photocatalytic CO_2 reduction test.

Table S6.TON of all products (CO and H2) and CO on LDH/TiC-1.7.

	TOF h^{-1}	TON ($CO+H_2$)	TON (CO)	AQY_{CO}(%)	ref
LDH/TiC-1.7	0.264	949	385	1.26	this work
Co1-GO	-	678	-	-	Adv. Mater., 2018, 30, 1704624[14].
Co-ZIF-9	-	89.6	-	1.48	Angew. Chem. Int. Ed., 2014, 53, 1034-1038[15].

The TON level and AQY_{co} is comparable with other advanced heterogeneous catalytic systems in the literatures. The turnover frequency (TOF) was defined as the moles of produced product per mole of catalytic sites per hour. (Catalytic active sites are Co and TiC; Catalytic active sites Co+TiC =0.069 mmol; TON = TOF*t)

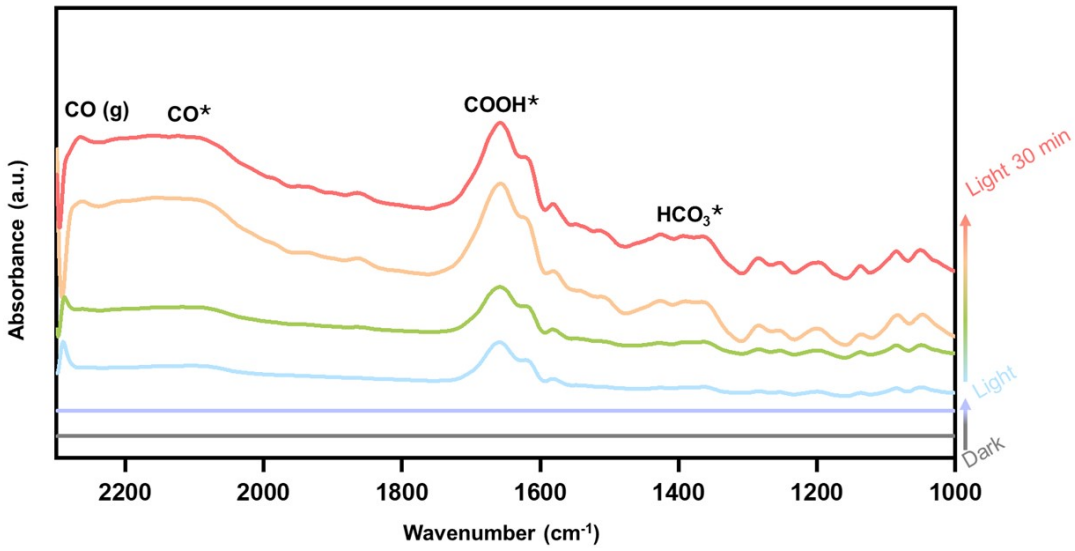

Figure S13. *In-situ* FTIR spectra of LDH/TiC-1.2 during CO_2 reduction under visible light irradiation.

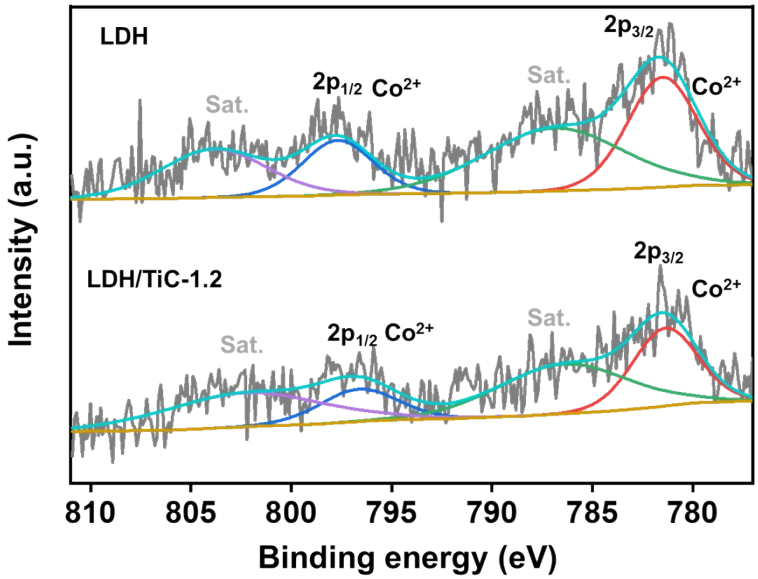

Figure S14. Co 2p X-ray photoelectron spectroscopy (XPS) of LDH and LDH/TiC-1.2, respectively.

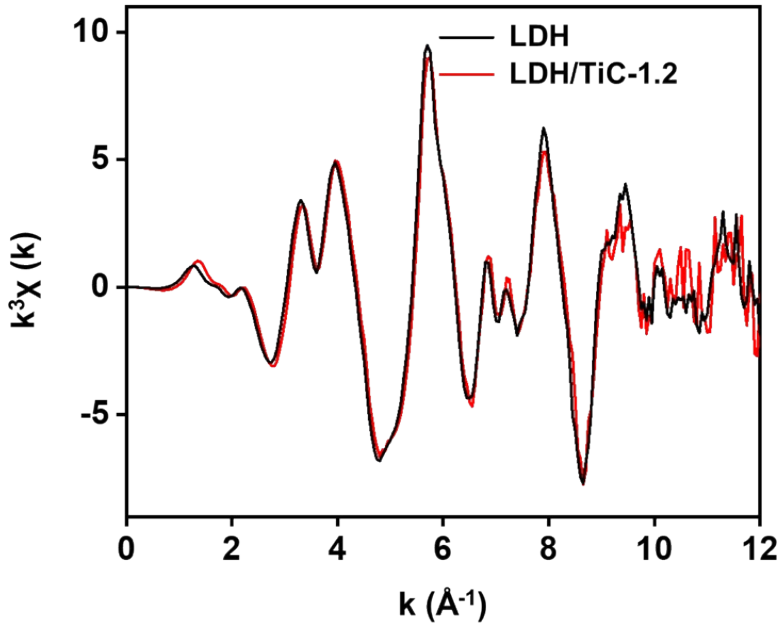

Figure S15. Co *K*-edge EXAFS oscillation functions $k^3\chi(k)$ for LDH and LDH/TiC-1.2.

Table S7. Local structure parameters around Co in LDH and LDH/TiC-1.2 estimated by EXAFS analysis.

Sample	Shell	N^a	R[Å]^b	ΔE_0(eV)$_c$	σ^2[10^{-3}Å^2]^c	R-factor(10^{-2})
LDH	Co-O	5.9	2.09	-1.02	7.13	1.09
	Co-Mg/Al	5.1	3.07	1.05	5.39	
LDH/TiC-1.2	Co-O	5.7	2.09	0.26	8.12	1.20
	Co-Mg/Al	5.0	3.07	2.18	6.25	

^{a}N = coordination number; ^{b}R = distance between absorber and backscatter atoms; $^c\Delta E_0$: the inner potential correction; $^c\sigma^2$ = Debye-Waller factor.

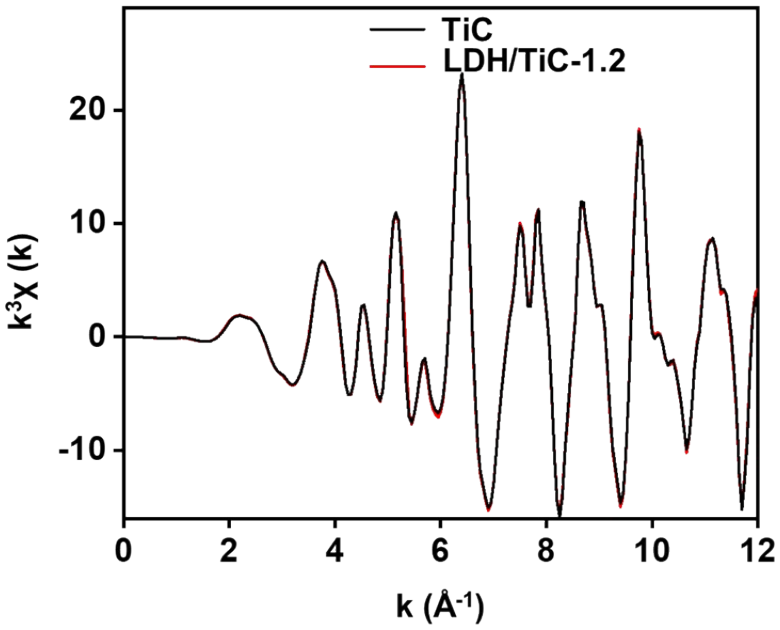

Figure S16. Ti *K*-edge EXAFS oscillation functions $k^3\chi(k)$ for LDH/TiC-1.2 and TiC.

Table S8. Local structure parameters around Ti in LDH/TiC-1.2 and TiC estimated by EXAFS analysis.

Sample	Shell	N^a	R[Å]^b	ΔE_0(eV)^c	σ^2[10^{-3}Å^2]^c	R-factor(10^{-2})
TiC	Ti-C	6.0	2.17	-1.64	4.00	0.50
	Ti-Ti	12.0	3.05	-7.90	3.20	
LDH/TiC-1.2	Ti-C	5.9	2.16	-2.90	4.06	0.60
	Ti-Ti	11.9	3.05	-7.61	3.08	

^{a}N = coordination number; ^{b}R = distance between absorber and backscatter atoms; $^c\Delta E_0$: the inner potential correction; $^c\sigma^2$ = Debye-Waller factor.

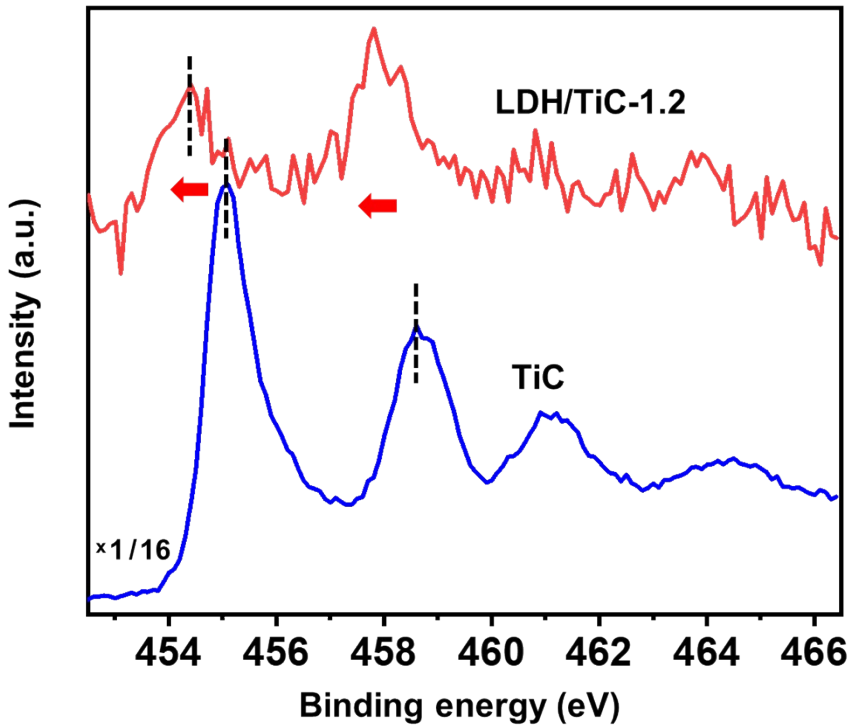

Figure S17. Ti 2p X-ray photoelectron spectroscopy (XPS) of LDH/TiC-1.2 and TiC, respectively.

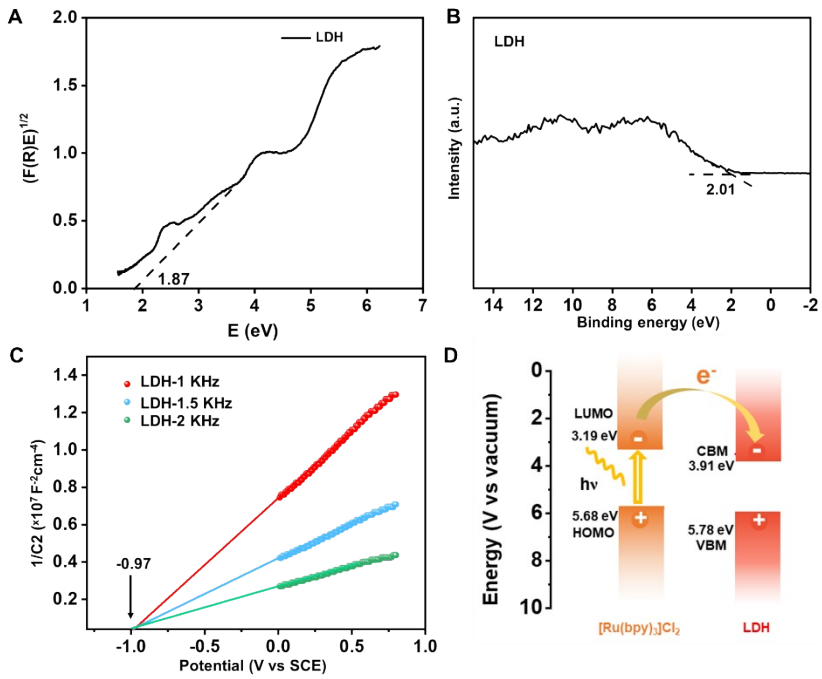

Figure S18. A) The bandgaps calculated for LDH; B) The valance band XPS spectra of LDH; C) Mott-Schottky plots of LDH; D) Schematic energy-level diagram showing electron transfer from $[Ru(bpy)_3]Cl_2$ to LDH. (CBM: conduction band minimum; VBM: valence band maximum; LUMO: lowest unoccupied molecular orbital; HOMO: highest occupied molecular orbital.)

In order to further explore the reaction mechanism, we calculated the band structure of LDH. As shown in Figure S18A, it band gap energy was 1.87 eV. Furthermore, the relative position of valance band maximum (VBM) to the Fermi level (E_f) was determined by valance band XPS spectra (Figure S16B), the VBM positions of LDH was estimated to be 2.01 eV, below the Fermi level. And the flat band potential of LDH was -0.97 V vs. saturated calomel electrode (SCE) (Figure S18C). Thus, the band structures relative to the normal hydrogen electrode (NHE) at pH 7 were summarized in Figure S18D the conduction band minimum (CBM) of LDH (3.91 eV) was lower than the LUMO of $[Ru(bpy)_3]Cl_2$ (3.19 eV) so that the photoexcited electrons in the LUMO of photosensitizer can be preferentially transferred to the CBM of LDH, enabling the subsequent reduction of CO_2, thereby promoting the catalytic reaction[16].

Table S9. Reduction potentials of CO_2[17].

Reaction	E_0 (V) vs. NHE at pH 7
$2H^+ + 2e^- \rightarrow H_2$	-0.41
$CO_2 + e^- \rightarrow CO_2^-$	-1.9
$CO_2 + 2H^+ + 2e^- \rightarrow HCO_2H$	-0.61
$CO_2 + 2H^+ + 2e^- \rightarrow CO + H_2O$	-0.53

References

1. S. Wang, W. Yao, J. Lin, Z. Ding and X. Wang, *Angew. Chem. Int. Ed.*, 2014, **53**, 1034-1038.
2. C. Gao, Q. Meng, K. Zhao, H. Yin, D. Wang, J. Guo, S. Zhao, L. Chang, M. He, Q. Li, H. Zhao, X. Huang, Y. Gao and Z. Tang, *Adv. Mater.*, 2016, **28**, 6485-6490.
3. T. Ouyang, H.-H. Huang, J.-W. Wang, D.-C. Zhong and T.-B. Lu, *Angew. Chem. Int. Ed.*, 2017, **56**, 738-743.
4. Y. Wang, N.-Y. Huang, J.-Q. Shen, P.-Q. Liao, X.-M. Chen and J.-P. Zhang, *J. Am. Chem. Soc.*, 2018, **140**, 38-41.
5. C. Gao, S. Chen, Y. Wang, J. Wang, X. Zheng, J. Zhu, L. Song, W. Zhang and Y. Xiong, *Adv. Mater.*, 2018, **30**, 1704624.
6. K. Zhao, S. Zhao, C. Gao, J. Qi, H. Yin, D. Wei, M. F. Mideksa, X. Wang, Y. Gao, Z. Tang and R. Yu, *Small*, 2018, **14**, 1800762.
7. X. Wang, Z. Wang, Y. Bai, L. Tan, Y. Xu, X. Hao, J. Wang, A. H. Mahadi, Y. Zhao, L. Zheng and Y.-F. Song, *J. Energy. Chem.*, 2020, **46**, 1-7.
8. M. Liu, Y.-F. Mu, S. Yao, S. Guo, X.-W. Guo, Z.-M. Zhang and T.-B. Lu, *Appl. Catal., B*, 2019, **245**, 496-501.
9. T. Fogeron, P. Retailleau, L.-M. Chamoreau, Y. Li and M. Fontecave, *Angew. Chem. Int. Ed.*, 2018, **57**, 17033-17037.
10. J. Qin, S. Wang, H. Ren, Y. Hou and X. Wang, *Appl. Catal., B*, 2015, **179**, 1-8.
11. C. Qiu, X. Hao, L. Tan, X. Wang, W. Cao, J. Liu, Y. Zhao and Y.-F. Song, *Chem. Commun.*, 2020, **56**, 5354-5357.
12. K. Teramura, S. Iguchi, Y. Mizuno, T. Shishido and T. Tanaka, *Angew. Chem. Int. Ed.*, 2012, **51**, 8008-8011.
13. Z. Wang, S.-M. Xu, L. Tan, G. Liu, T. Shen, C. Yu, H. Wang, Y. Tao, X. Cao, Y. Zhao and Y.-F. Song, *Appl. Catal., B*, 2020, **270**.
14. C. Gao, S. Chen, Y. Wang, J. Wang, X. Zheng, J. Zhu, L. Song, W. Zhang and Y. Xiong, *Adv. Mater.*, 2018, **30**, 1704624
15. S. Wang, W. Yao, J. Lin, Z. Ding and X. Wang, *Angew. Chem. Int. Ed.*, 2014, **53**, 1034-1038.
16. C. Ning, Z. Wang, S. Bai, L. Tan, H. Dong, Y. Xu, X. Hao, T. Shen, J. Zhao, P. Zhao, Z. Li, Y. Zhao and Y.-F. Song, *Chem. Eng. J.*, 2021, **412**, 128362.
17. X. Li, J. Wen, J. Low, Y. Fang and J. Yu, *Science China Materials*, 2014, **57**, 70-100.